Geochemistry of the Quaternary alkali basalts of Garrotxa (NE Volcanic Province, Spain): a case of double enrichment of the mantle lithosphere

J.M. Cebriá[a,*], J. López-Ruiz[a], M. Doblas[a], R. Oyarzun[b], J. Hertogen[c], R. Benito[a]

[a]*Departamento de Geología, Museo Nacional de Ciencias Naturales (CSIC), José Gutierrez Abascal 2, 28006 Madrid, Spain*
[b]*Departamento de Mineralogía y Cristalografía, Facultad de Ciencias Geológicas, Universidad Complutense de Madrid, 28040 Madrid, Spain*
[c]*Fysico-Chemische Geologie, Universiteit Leuven, 3001 Leuven, Belgium*

Abstract

The area of Garrotxa (also known as the Olot area) represents the most recent (700,000–11,500 y) and better preserved area of magmatic activity in the NE Volcanic Province of Spain (NEVP). This region comprises a suite of intracontinental leucite basanites, nepheline basanites and alkali olivine basalts, which in most cases represent primary or nearly primary liquids. The geochemical characteristics of these lavas are very similar to the analogous petrologic types of other Cenozoic volcanics of Europe, which are intermediate between HIMU, DM and EM1.

Quantitative trace element modeling, suggests derivation from an enriched mantle source by degrees of melting that progressively increased from the leucite basanites (~4%) to the olivine basalts (~16%). However, the relatively more variable Sr–Nd–Pb isotope signature of the magmas suggests the participation of at least two distinct components in the mantle source: (1) a sublithospheric one with a geochemical signature similar to the magmas of Calatrava (Central Spain) and other basalts of Europe; and (2) an enriched lithospheric component with a K-bearing phase present. The geochemical model proposed here involves the generation of a hybrid mantle lithosphere source produced by the infiltration of the sublithospheric liquids into enriched domains of the mantle lithosphere, shortly before the melting event that generated the Garrotxa lavas.

The available geological data suggest that the first enrichment event of the mantle lithosphere under the NEVP could be the result of Late Variscan mantle upwelling triggered by the extensional collapse of the Variscan orogen during the Permo-Carboniferous. By Jurassic/Cretaceous time, large-scale NNE-directed sublithospheric mantle channeling of thermally and chemically anomalous plume material was placed under the Iberian Peninsula and Central Europe. However, the geodynamic conditions in the NEVP did not favor magmatism, which could not take place until the Cenozoic after extension started. This favored the second enrichment event of the mantle lithosphere by entrainment and storage of liquids generated in the sublithospheric plume material. After a relatively short period of time, as extension progressed, it triggered melting in the enriched portions of the mantle lithosphere during the Quaternary, generating the Garrotxa volcanism.

Keywords: mantle lithosphere; metasomatism; partial melting; trace element modeling; NE Volcanic Province of Spain; European Cenozoic volcanism

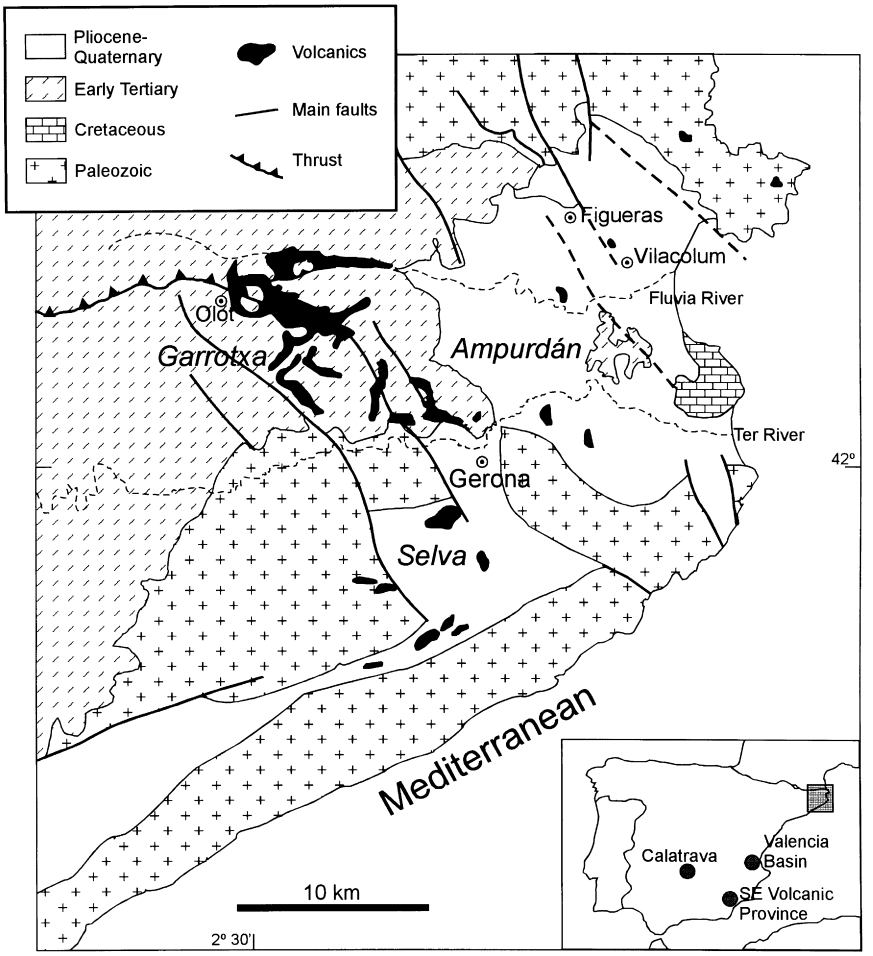

Fig. 1. Simplified geological map of the volcanic region of NE Spain (modified from Guérin et al., 1986). The inset also shows the location of the other Neogene-Quaternary volcanic areas of Spain.

1. Introduction

Following the Alpine compressions, the Iberian realm was subjected to extensional conditions (e.g. Doblas and Oyarzun, 1989, 1990) giving rise to a series of basins which in some cases were the site of magmatism. The volcanic activity concentrated in four main provinces (see Fig. 1): The NE Volcanic Province (NEVP), the Valencia Basin, Calatrava, and the SE Volcanic Province.

The NEVP developed in a series of extensional basins and minor graben-type structures hosting intraplate alkaline basaltic volcanism with close affinities to the analogous Tertiary/Quaternary intraplate magmatism of the neighboring volcanic provinces of Calatrava, Central Spain (López-Ruiz et al., 1993; Cebriá and López-Ruiz, 1995) and Massif Central, France (Chauvel and Jahn, 1984; Downes, 1984; Briot et al., 1991; Wilson and Downes, 1991; Wilson et al., 1995a), as well as the Volcanic Provinces of Germany (Mertes and Schmincke, 1985; Wörner et al., 1986; Wilson and Downes, 1991; Wedepohl et al., 1994; Hegner et al., 1995; Wilson et al., 1995b; Jung and Masberg, 1998), thus linking this volcanism to the European Cenozoic extension-related magmatism.

The lavas of the NEVP have previously been studied from both the petrologic and geochemical point of view (mainly Araña et al., 1983; López-Ruiz

and Rodríguez-Badiola, 1985) as well as from the geotectonic one (Araña et al., 1983; Zeyen et al., 1991; Martí et al., 1992). Although several geodynamic hypotheses have been suggested for the volcanism of the NEVP, the previously available models for the geochemical evolution of the region were insufficient and therefore the proposed geodynamic/geochemical models could not satisfactorily integrate the geological, structural, and geochemical data within a global tectonomagmatic scheme. In this work, we present the first comprehensive isotopic (Sr–Nd–Pb) and major and trace element study of the Quaternary volcanism in this area, which is concentrated in the sector of Garrotxa. This sector is the best preserved in the NEVP and it is considered as representative of the whole region from a petrologic and geochemical point of view (López-Ruiz and Rodríguez-Badiola, 1985). Most of the lavas in this area show the characteristics usually attributed to primary magmas thus making them ideal candidates to constrain the composition of their mantle source. Following the quantitative trace element modeling of the partial melting process, we will integrate the results of this approach with other geochemical and geological observations to better understand the magmatic/geodynamic evolution of this volcanic region in connection to the related volcanism of Europe.

2. General characteristics of the volcanism

The NEVP consists of some 200 volcanic outcrops irregularly distributed in an area of ca. 2500 km^2 located to the south of the Pyrenees (Fig. 1). This region is usually divided into three main areas (Garrotxa – also known as the Olot area, Ampurdán and Selva) that correspond to tectonic basins originated during extensional processes in the Middle Miocene (Serravallian) (Solé-Sugrañés et al., 1984). The volcanism is represented by some well-preserved strombolian cones and lava flows. The erosion of the older manifestations has produced numerous pyroclastic deposits, isolated basaltic outcrops and necks. Hydromagmatic deposits are also found in the area (Martí and Mallarach, 1987).

The available K/Ar ages (Donville, 1973a,b,c; Araña et al., 1983) indicate that magmatism started shortly after the opening of the neogene basins in Ampurdán (10–9 Ma), continued in Selva (7–2 Ma) and finished in Garrotxa (0.7–0.11 Ma). Although the general evolution of the volcanism, deduced from K/Ar dating, is probably valid in a general sense, the time-span for the activity in each area is likely to be wider. For example, dates based on thermoluminescence of plagioclases for the area of Garrotxa (Guérin et al., 1986) indicate a lower age limit of 11,500 y. The younger character of the volcanism in the Garrotxa area, explains the presence of a higher number of outcrops (≈ 100) which are the best preserved in the region (about 50 correspond to cinder cones).

The general variation observed in the absolute ages seems to be related to the relative opening of the basins from the external areas (Ampurdán and Selva) to Garrotxa (Araña et al., 1983). In general, the volcanic vents are related to a complex faulting system dominated by NW–SE and SW–NE directions (Solé-Sabarís, 1962; Solé-Sugrañés, 1978; Araña et al., 1983).

3. Analytical procedures

Whole-rock samples were analyzed for major elements (Si, Ti, Al, Total Fe, Mn, Mg, Ca, K and P) by XRF on fused glass disks on an automated Philips PW-1410/20 system, with Cr and W X-ray tubes at the Museo Nacional de Ciencias Naturales (CSIC, Madrid). The ferrous iron content was determined by manganometric titration. Atomic absorption flame spectrometry (on a Perkin–Elmer 2320 spectrometer) was used to analyze Na over dry digestion with HNO_3+HClO_4+HF and HCl extraction.

Concentrations of Sc, Cr, Co, Ba, REE, Hf, Ta, Pb, Th and U in whole-rock samples were obtained by INAA, and Zn, Rb, Sr, Y and Nb by XRF on pressed powder pellets, at Leuven University (Belgium). The analyses were performed using standard procedures relative to a secondary basalt standard, which has been repeatedly calibrated against the BCR-1 reference rock.

Sr and Nd isotopic ratios were measured on ~200 mg of whole rock powders. To eliminate the possible modification of the original ratios due to secondary alteration, the samples were leached for

Table 1
Major and trace element (in % and ppm, respectively), and isotopic composition of the basaltic rocks from Garrotxa (NE Volcanic Province, Spain)

	Leucite basanites							
	GA-8	GA-7	GA-15	GA-13	GA-16	GA-1	GA-20	GA-6
SiO_2	42.97	43.58	43.65	44.05	44.28	44.67	44.68	45.93
TiO_2	2.51	2.32	2.85	2.32	2.33	2.10	2.57	2.10
Al_2O_3	14.82	14.27	14.06	13.07	13.18	14.05	15.81	14.16
Fe_2O_3	4.39	5.48	3.28	4.46	5.18	3.16	2.72	5.32
FeO	6.99	5.93	7.35	7.02	6.21	8.60	7.08	6.38
MnO	0.19	0.18	0.21	0.21	0.20	0.19	0.18	0.19
MgO	9.08	8.95	10.98	9.88	9.88	8.68	8.86	7.50
CaO	10.74	10.32	8.93	9.72	9.92	10.47	9.65	9.79
Na_2O	3.80	3.74	4.15	4.50	4.33	3.74	4.13	4.19
K_2O	2.21	2.40	2.11	2.49	2.31	1.90	2.13	2.49
P_2O_5	0.59	0.65	0.84	0.84	0.85	0.66	0.60	0.57
L.O.I.	1.53	1.62	1.52	1.27	1.15	1.38	1.48	1.31
Total	99.82	99.44	99.93	99.83	99.82	99.60	99.89	99.93
Rb	58	50	63	72	72	50	70	57
Ba	776	880	877	911	992	797	829	880
Sr	843	870	1037	1117	1100	922	953	1018
La	49.0	52.0	71.6	79.6	81.4	50.1	58.7	65.3
Ce	103	98	147	162	166	104	119	127
Nd	45.0	–	63.0	66.0	68.0	47.6	48.2	51.7
Sm	8.2	–	10.3	10.8	11.2	8.5	8.3	8.8
Eu	2.53	–	3.11	3.20	3.29	2.69	2.61	2.71
Tb	0.99	–	1.15	1.19	1.20	1.02	0.98	1.02
Yb	2.13	–	2.28	2.39	2.51	2.11	2.19	2.21
Lu	0.30	–	0.35	0.40	0.38	0.29	0.32	0.32
Y	23	23	27	29	27	24	24	25
Zr	233	220	283	331	390	220	248	265
Hf	5.3	–	6.2	7.0	8.2	5.1	5.5	5.7
Nb	77	–	112	123	120	78	95	104
Ta	4.43	–	6.40	7.00	6.70	4.43	5.70	6.10
Pb	7	6	8	8	10	4	–	8
Th	5.6	7.0	8.0	8.9	9.3	5.1	6.4	6.5
U	1.5	–	2.0	2.3	2.4	1.4	1.7	1.6
Sc	25.5	–	18.4	17.0	19.2	24.5	21.4	20.1
V	263	273	264	220	239	218	235	205
Cr	140	195	317	338	227	211	168	167
Co	50.1	22.0	48.4	43.0	43.3	49.2	43.2	40.2
Ni	135	83	319	270	288	86	125	90
Cu	44	41	22	23	28	41	38	40
Zn	84	n.d.	81	95	98	75	89	88
$\delta^{18}O^{a}$	–	–	6.12	6.53	–	–	–	6.31
$^{87}Sr/^{86}Sr$	0.703801 ± 12	–	0.703619 ± 26	0.703684 ± 14	0.703792 ± 10	–	–	0.703583 ± 12
$^{143}Nd/^{144}Nd$	0.512770 ± 24	–	0.512729 ± 24	0.512749 ± 24	0.512714 ± 20	–	–	0.512727 ± 34
$^{206}Pb/^{204}Pb$	18.88	–	19.47	–	–	–	–	19.19
$^{207}Pb/^{204}Pb$	15.60	–	15.65	–	–	–	–	15.63
$^{208}Pb/^{204}Pb$	38.64	–	39.26	–	–	–	–	38.94

1 h in warm 2.5 M HCl in sealed PFA Teflon® beakers. The leached residues were then dried down and digested in concentrated HNO_3 + HF for 48 h minimum. Conventional cation exchange procedures were then followed to obtain Sr and Nd. Pb isotopic ratios were measured on aliquots of ~200 mg of sample. Leaching procedures were the same followed for Sr and Nd and standard cation exchange procedures were also followed. Strontium was analyzed on a VG 54E Isomass spectrometer, and Nd and Pb were

Table 1 (*continued*)

	Basanites						Olivine Basalts	
	GA-11	GA-9	GA-12	GA-5	GA-18	GA-19	GA-17	GA-2
SiO_2	41.60	43.13	43.82	45.74	46.58	46.60	46.98	49.28
TiO_2	2.43	2.54	2.68	2.25	2.35	2.32	2.60	2.34
Al_2O_3	14.82	13.83	13.17	14.05	16.24	16.30	15.95	14.49
Fe_2O_3	4.45	5.13	4.39	3.36	2.78	3.36	2.97	2.70
FeO	8.14	7.20	7.90	8.18	7.62	7.20	7.29	7.33
MnO	0.20	0.19	0.20	0.20	0.16	0.16	0.17	0.19
MgO	9.79	9.65	9.45	8.02	7.30	7.05	7.16	7.32
CaO	10.51	10.74	11.07	10.01	9.76	9.75	9.60	9.05
Na_2O	3.67	3.52	3.87	3.92	3.74	4.03	3.81	3.98
K_2O	1.72	1.76	1.52	1.71	1.40	1.42	1.39	1.72
P_2O_5	0.56	0.61	0.62	0.48	0.49	0.45	0.50	0.45
L.O.I.	1.80	1.50	1.28	1.62	1.52	1.31	1.22	1.13
Total	99.69	99.80	99.97	99.54	99.94	99.95	99.64	99.98
Rb	30	40	37	36	28	30	28	43
Ba	651	707	690	634	504	482	500	673
Sr	706	826	863	793	745	708	704	703
La	33.6	43.9	43.1	41.6	37.1	36.7	36.6	40.3
Ce	72	95	93	88	79	78	78	83
Nd	35.8	45.5	44.1	38.2	36.6	35.5	35.1	36.6
Sm	7.2	8.0	8.3	7.3	7.0	6.9	6.9	6.8
Eu	2.34	2.51	2.64	2.38	2.29	2.27	2.25	2.18
Tb	0.97	0.96	1.05	0.98	0.93	0.92	0.91	0.87
Yb	1.87	2.02	2.05	2.07	1.92	1.92	1.92	1.92
Lu	0.24	0.28	0.32	0.30	0.29	0.29	0.29	0.30
Y	22	22	23	22	21	21	22	22
Zr	165	186	185	200	174	174	175	221
Hf	4.2	4.4	4.6	4.9	4.3	4.3	4.2	4.8
Nb	52	71	66	66	55	53	56	67
Ta	3.09	4.17	3.96	3.99	3.39	3.37	3.36	4.10
Pb	6	10	6	7	5	7	–	6
Th	2.91	4.29	3.68	4.12	3.70	3.74	3.71	4.43
U	0.72	1.07	0.93	1.09	0.73	0.99	0.98	1.21
Sc	25.3	25.6	24.3	21.8	21.9	21.6	21.9	18.6
V	267	277	262	210	220	196	207	193
Cr	210	176	170	190	159	144	164	200
Co	55.8	54.8	52.8	47.4	42.9	41.4	42.1	42.7
Ni	142	145	122	107	75	69	67	103
Cu	42	45	44	44	46	41	41	45
Zn	92	94	91	89	91	82	99	93
$\delta^{18}O$[a]	6.27	5.62	–	–	–	–	–	–
$^{87}Sr/^{86}Sr$	0.703587 ± 10	0.703594 ± 12	0.703627 ± 12	0.703627 ± 8	–	–	0.703603 ± 22	0.703676 ± 12
$^{143}Nd/^{144}Nd$	0.512786 ± 24	0.512726 ± 24	0.512719 ± 26	0.512833 ± 30	–	–	0.512729 ± 26	0.512748 ± 28
$^{206}Pb/^{204}Pb$	19.01	19.00	–	19.23	–	–	19.24	19.15
$^{207}Pb/^{204}Pb$	15.62	15.59	–	15.64	–	–	15.68	15.62
$^{208}Pb/^{204}Pb$	38.79	38.68	–	38.96	–	–	39.16	38.84

[a] After Benito-García et al. (1992).

analyzed on a VG MM30 mass spectrometer, both at the Geochronology Laboratory of the School of Earth Sciences (University of Leeds, UK). Nd isotopic compositions were normalized to $^{146}Nd/^{144}Nd = 0.7219$ relative to La Jolla standard ($^{143}Nd/^{144}Nd = 0.511897 \pm 18$), and Sr isotopic compositions were normalized to $^{87}Sr/^{86}Sr = 0.1194$ relative to SRM 987 standard ($^{87}Sr/^{86}Sr = 0.7102927 \pm 10$). All Pb analyses were corrected for mass fractionation by 0.47‰ amu^{-1}, based on 10 replicate runs of SRM

981, which gave $^{208}Pb/^{206}Pb = 2.16475 \pm 0.00071$, $^{207}Pb/^{206}Pb = 0.914250 \pm 0.000152$ and $^{204}Pb/^{206}Pb = 0.059095 \pm 0.000026$.

4. Petrology and geochemistry of the basaltic rocks

On the basis of their modal and normative mineralogy, the volcanic rocks of the NEVP can be divided into four groups (López-Ruiz and Rodríguez-Badiola, 1985): leucite basanites (LBAS), nepheline basanites (NBAS), alkali olivine basalts (AOB) and trachytes (TR).

The TR are restricted to a few outcrops in the Ampurdán area that might represent the remains of volcanic necks and show variable but strong degrees of alteration. Their mineralogy is mainly represented by phenocrysts of plagioclase (andesine–oligoclase) and occasionally of phlogopite, amphibole and apatite embedded in a groundmass of feldspar and Fe–Ti oxides (López-Ruiz and Rodríguez-Badiola, 1985; Díaz et al., 1996).

The LBAS, NBAS and AOB are found in all the areas of the NEVP, although the LBAS appear almost exclusively in Garrotxa. The three groups have very similar mineralogy. All rocks are porphyritic with olivine (Fo_{90-74}) and clinopyroxene (En_{52-30}–Fs_{4-23}–Wo_{43-51}) as phenocrysts and a groundmass constituted by plagioclase (An_{71-61}, which can also appear as microphenocrysts), titanomagnetite, leucite and nepheline. The presence of mantle xenoliths is also a common feature in all groups. The only significant differences are the higher abundance of leucite in the LBAS and the presence of analcime in the groundmass of the NBAS. The mineral chemistry is also analogous in all groups and the compositional variations observed in Garrotxa cover the full range for the NEVP (see López-Ruiz and Rodríguez-Badiola, 1985). The only apparent regional variations can be attributed to variable alteration degrees, which in general are higher in the older rocks (i.e. those of Ampurdán and Selva). For these reasons, the geochemical discussion is focused on the rocks from Garrotxa which are the freshest in the NEVP and that, excluding the TR, can be considered as representative for the whole region (López-Ruiz and Rodríguez-Badiola, 1985).

4.1. Major and trace elements

Most lavas from Garrotxa have $Na_2O + K_2O > 5\%$ and high proportions of MgO, TiO_2 and P_2O_5, and mg# = 57.7–68.3, typical of relatively primitive alkali basalts. This character is supported by the occasional presence of peridotite xenoliths. The LBAS are characterized by higher K_2O values (>1.9%) relative to NBAS and AOB ($K_2O < 1.76\%$), which cannot be readily distinguished on the basis of their major element composition except for a slightly higher SiO_2 abundance in the AOB (Table 1).

The major elements vs. MgO diagrams (Fig. 2) show that in general the three groups follow coherent patterns of depletion in SiO_2 and Al_2O_3 and enrichment in MnO and P_2O_5 as well as a noticeable scattering in TiO_2. The apparent dispersion in Na_2O and CaO is caused by the scattering of the LBAS, which depart from otherwise usual trends of enrichment in CaO and depletion in Na_2O relative to MgO. The LBAS systematic high content in K_2O also masks a slight tendency to enrichment relative to SiO_2.

Normalized trace element diagrams for these lavas are presented in Fig. 3. All groups show analogous patterns, characterized by variable enrichment degrees relative to primitive mantle concentrations, being lowest for Y and Yb ($\times 4$–5) and highest for Ba and Nb–Ta, which display positive anomalies. There are no significant differences between the primary lavas and the slightly evolved ones, indicating that differentiation has played only a minor role in this series. The LBAS show the highest enrichment in all elements considered, whereas the ranges of NBAS and AOB overlap showing nearly identical patterns.

The only significant variations from the more enriched samples (represented by LBAS) to the less enriched ones (NBAS and AOB), is the progressively stronger negative Rb spike and the production of a negative spike in Th. Most of the samples show a small positive Zr anomaly, although it is very weak or even absent in the NBAS. The normalized diagram of Fig. 3 shows that the division between NBAS and AOB is only relatively consistent when considering their petrography and their major element composition, but it lacks significance when considering trace elements (and isotopic ratios, as we will show), so in fact they should be considered as a single group.

These trace element patterns are similar to those

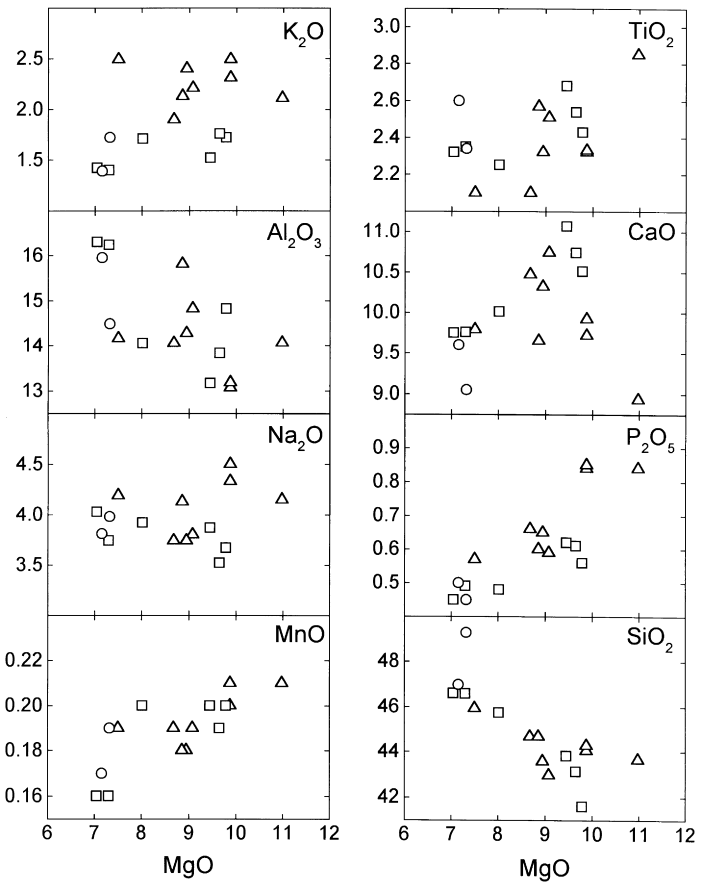

Fig. 2. MgO-major elements diagrams for the lavas of Garrotxa (triangles: leucite basanites; squares; nepheline basanites; circles: olivine basalts).

described for other Cenozoic lavas of Europe (see for example Chauvel and Jahn, 1984; Wilson and Downes, 1991; Wedepohl et al., 1994; Cebriá and López-Ruiz, 1995) which are typical of OIB lavas with HIMU-like characteristics, such as the positive Nb–Ta anomaly (e.g. St. Helena, Bouvet, Ascension; Weaver, 1991) and the negative one of Th (e.g. Tubuai; Chauvel et al., 1992). However, the strong positive Ba anomaly is not usually observed in HIMU patterns but is typical of some EM1 lavas (e.g. Gough; Weaver, 1991).

The nearly primary character of most of these rocks and the variations observed in Fig. 3 are in agreement with an origin by partial melting from a single enriched source. The lowest degrees of melting would produce the more enriched melts (LBAS) whereas the less enriched melts (NBAS and AOB) would be generated by the highest degrees of melting. As we will show, the relative differences in the distribution coefficients of the highly incompatible elements (e.g. Th, La, Ce) and the less incompatible elements can explain the variations observed in the normalized diagrams, such as the negative spike in Th, which is caused by the less incompatible behavior of K and Ba (thus showing very little variation with the degree of melting) relative to Th (which is highly incompatible). This relative buffering of K, Rb and Ba, and the absence of strong negative spikes for these elements, suggests the presence of small proportions of a potassic phase in the mantle residue (e.g.

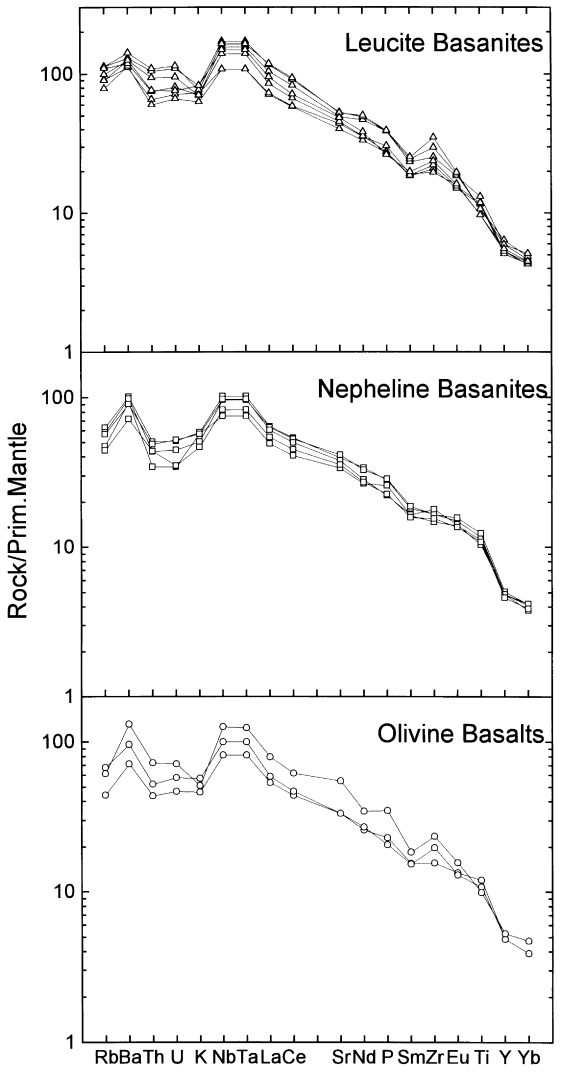

Fig. 3. Multi-element diagrams normalized relative to the Primitive Mantle (after Sun and McDonough, 1989) for the lavas of Garrotxa (symbols as in Fig. 2).

kaersutite or phlogopite) during the melting process. Additionally, the higher K_2O proportion of the LBAS when compared to NBAS and AOB, implies that this K-bearing phase has entered the liquid in higher amounts at the lowest degrees of melting.

Although the presence of garnet or spinel in the mantle source is difficult to establish, several observations suggest garnet as the more likely aluminous phase. For example, the strong fractionation of the HREE relative to the MREE (Eu/Yb = 1.14 − 1.36) are indicative of segregation of the magmas from the garnet domain. If this is correct, the relatively constant values of the Eu/Yb (1.25 ± 0.08) and CaO/Al_2O_3 (0.71 ± 0.07) ratios relative to Th, suggest that the participation of garnet during the melting process has remained nearly constant relative to clinopyroxene. However, we will see later that this inference must be taken with caution as these source characteristics can also be inherited from previous melting events.

4.2. Sr–Nd–Pb–O isotopes

The Sr–Nd–Pb isotopic characteristics of the Garrotxa lavas are shown in Figs. 4 and 5 where fields for other Cenozoic European volcanics are also included for comparison.

As shown in the trace element patterns and similarly to other contemporaneous basaltic rocks of Europe, the lavas of Garrotxa have a Sr–Nd–Pb signature intermediate between HIMU and EM1 (Fig. 4). However, although the lavas from Garrotxa are similar to some of the slightly K-rich lavas in the series of the Bohemian Massif in Germany and Massif Central in France, their $^{143}Nd/^{144}Nd$ and $^{206}Pb/^{204}Pb$ ratios have slightly lower values relative to $^{87}Sr/^{86}Sr$.

There are no significant variations between groups, with the LBAS covering the full range of $^{87}Sr/^{86}Sr$ and $^{206}Pb/^{204}Pb$. The $^{87}Sr/^{86}Sr$–$^{143}Nd/^{144}Nd$ diagram shows no strong correlation, with the Garrotxa lavas plotting into a relatively narrow field defined by the average values $^{87}Sr/^{86}Sr = 0.70365 \pm 7$ and $^{143}Nd/^{144}Nd = 0.51274 \pm 3$, slightly elongated between HIMU and EM1. These values are in agreement with the relatively low $\delta^{18}O$ values which show little variation from the average value of 6.17‰ ($\sigma = 0.34$, $n = 5$) (Benito-García et al., 1992). This value is similar to those considered as typical of intracontinental primary lavas (see, for example, Kyser, 1986; Harmon and Hoefs, 1995; Hoefs, 1997). Although it can be considered as representing the signature of the mantle source, its slightly higher value when compared to the nearly constant ratio observed in MORB (5.7 ± 0.2‰) indicates the participation of a relatively enriched source (Hoefs, 1997).

Despite the apparent lack of sharp linear relationships when considering $^{87}Sr/^{86}Sr$ and

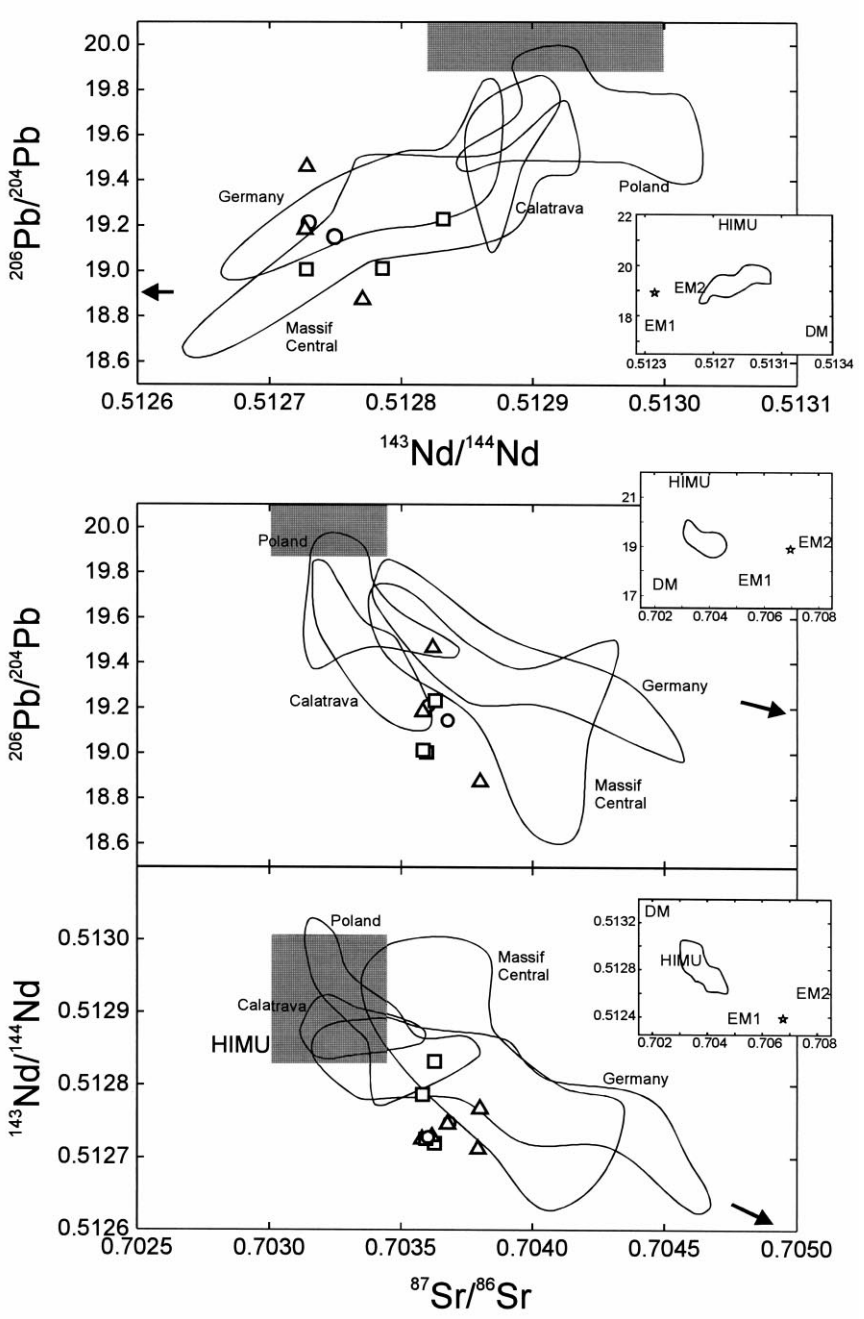

Fig. 4. $^{87}Sr/^{86}Sr$–$^{143}Nd/^{144}Nd$, $^{87}Sr/^{86}Sr$–$^{206}Pb/^{204}Pb$ and $^{143}Nd/^{144}Nd$–$^{206}Pb/^{204}Pb$ diagrams for the lavas of Garrotxa (symbols as in Fig. 2). The fields outline samples from Calatrava (unpublished data), Massif Central (Chauvel and Jahn, 1984; Downes, 1984; Briot et al., 1991; Wilson and Downes, 1991; Wilson et al., 1995a), German area basalts (Mertes and Schmincke, 1985; Wörner et al., 1986; Wilson and Downes, 1991; Wedepohl et al., 1994; Hegner et al., 1995; Wilson et al., 1995b), and Poland (Alibert et al., 1987; Blusztajn and Hart, 1989). The arrow points toward the composition of the Calatrava leucitites (see inset: star = Calatrava leucitites, field = Cenozoic European basalts). The shaded area corresponds to the field suggested for the LVC and EAR compositions (Hoernle et al., 1995; Cebriá and Wilson, 1995). The composition of the mantle reservoirs shown in the insets is from Zindler and Hart (1986) and Hart (1988).

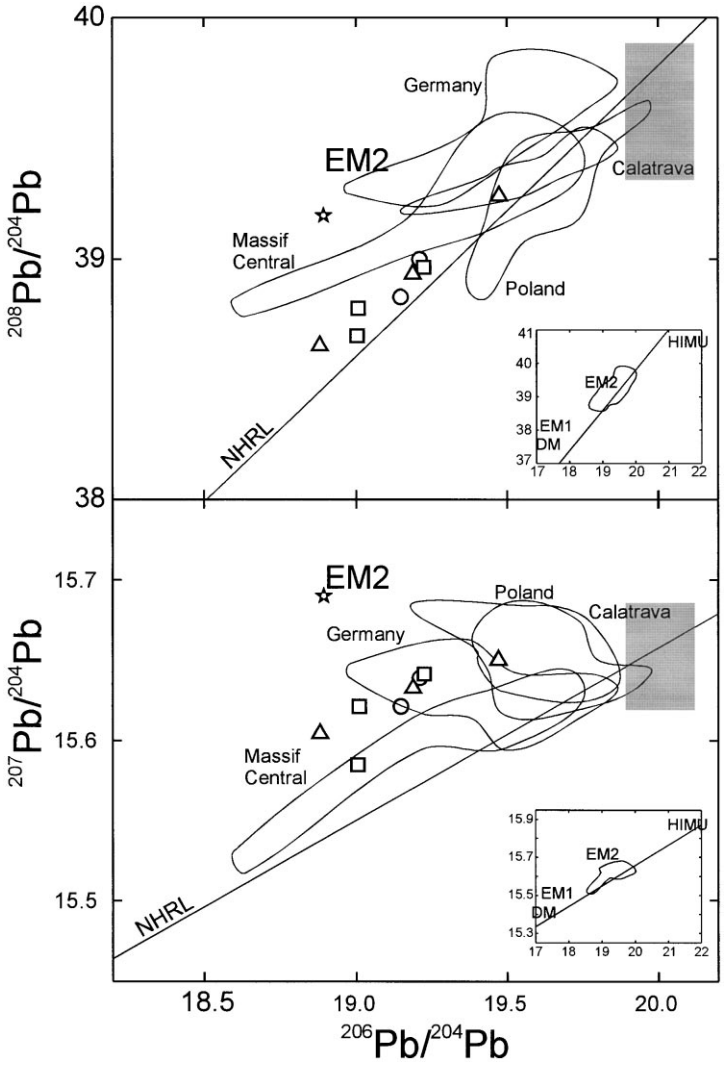

Fig. 5. $^{206}Pb/^{204}Pb$–$^{207}Pb/^{204}Pb$ and $^{206}Pb/^{204}Pb$–$^{208}Pb/^{204}Pb$ diagrams for the lavas of Garrotxa (symbols and data sources as in Fig. 4).

$^{143}Nd/^{144}Nd$, Pb isotopes show excellent correlations ($r = 0.83$ for $^{206}Pb/^{204}Pb$–$^{207}Pb/^{204}Pb$ and $r = 0.98$ for $^{206}Pb/\ ^{204}Pb$–$^{208}Pb/^{204}Pb$) nearly parallel to the NHRL but relatively enriched in $^{207}Pb/^{204}Pb$ and slightly in $^{208}Pb/^{204}Pb$, again in intermediate positions between HIMU and EM1 (Fig. 5). As we will show, although this variation could be interpreted as a secondary isochron of 1.57 Ga ($\kappa = 3.706$), it is more likely that it represents the interaction of two compositionally distinct components.

5. Petrogenetic model

As we have seen, the trace element patterns of the lavas of Garrotxa suggest that they are the result of partial melting from a single enriched mantle source. However, the slightly Sr-enriched signature of these basalts could also be the result of other processes such as crustal contamination. In continental areas such as the NEVP, recent contamination at crustal levels should modify several sensitive parameters, such as

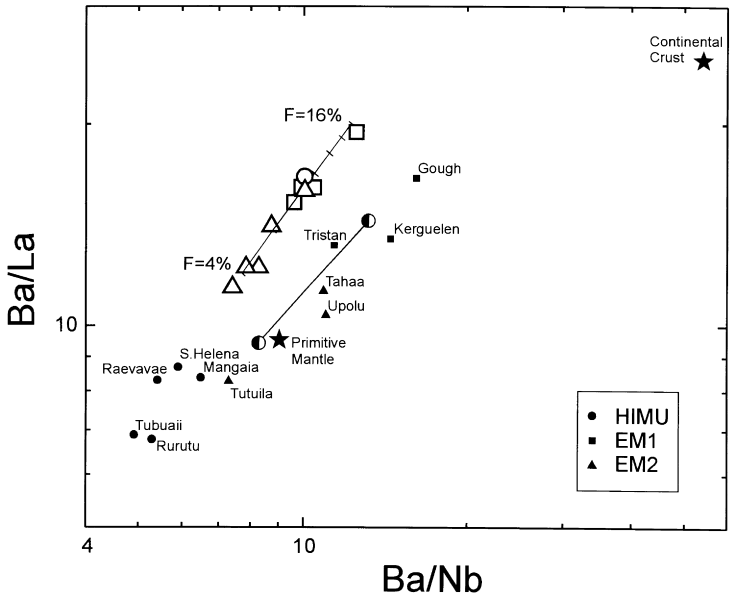

Fig. 6. Logarithmic Ba/Nb–Ba/La diagram (after Weaver, 1991) for the lavas of Garrotxa (symbols as in Fig. 2). The melting path from 4 to 16% corresponds to the model calculated in this work. The composition of the primitive mantle, continental crust and oceanic island basalts are from Weaver (1991). The second path (between half-filled circles) is a theoretical non-modal batch melting line calculated assuming the same melting range from an hydrous mantle assemblage, composed of 55%O1+20%Opx+15%Cpx+8%Gt+2%Phl, that melts in the proportions 10%O1+15%Opx+30%Cpx+15%Gt+30%Ph1. The initial trace element composition (in ppm) is Ba = 0.63, Nb = 0.233, and La = 0.25. The mineral/liquid distribution coefficients used for this calculation are those compiled by Halliday et al., (1995). This theoretical line shows that under hydrous conditions melting produces linear trends in this trace-element ratios diagram, similar to the one calculated for Garrotxa.

the $^{87}Sr/^{86}Sr$ and $\delta^{18}O$ ratios, and certain trace element ratios. Plots of $^{87}Sr/^{86}Sr$ versus 1/Sr or SiO_2 show no correlation ($r = 0.3$ and 0.6, respectively) and thus do not support the possibility of crustal contamination. Similarly, the lack of correlation between $^{87}Sr/^{86}Sr$ and $\delta^{18}O$ rules out crustal contamination and suggests that the slightly high $\delta^{18}O$ ratios (when compared to MORB) are a characteristic of this enriched mantle source. The use of binary diagrams based on incompatible trace element ratios such as the Ba/Nb–Ba/La (Weaver, 1991; Vidal, 1992) has also been suggested to discriminate mantle components and to identify the participation of components enriched in Ba and relatively depleted in Nb (e.g. continental crust). As it can be observed in Fig. 6, the lavas from Garrotxa plot in this diagram along a linear array starting at a position close to the HIMU magmas and pointing towards Ba-enriched compositions, a situation also observed in the neighbor province of Calatrava (Cebriá and López-Ruiz, 1995). However, although this could be interpreted as a mixing array between a HIMU-like source and an enriched component, in this particular case this variation can be reproduced by different degrees of partial melting due to the slightly different behavior of the elements involved (see Section 5.1 and Table 2). Nevertheless, the position of this array still suggests that, as observed in their trace element and isotope signature, the mantle source of the lavas of Garrotxa shows intermediate characteristics between HIMU and EM1.

The results of these tests and the observations made for all their other geochemical characteristics (homogeneity of the trace element patterns, mantle-like isotopic signature, presence of mantle xenoliths …) strongly support that the primary lavas of Garrotxa are the result of partial melting from a single source that is isotopically heterogeneous.

5.1. Trace element partial melting model

To obtain a quantitative model for the partial melting process responsible for the generation of the

Table 2
Values of the parameters obtained for the partial-melting model for the primary magmas from Garrotxa (NE Volcanic Province, Spain) (D_0: bulk distribution coefficient of the elements for the source paragenesis; P_L: Bulk distribution coefficient of the elements for the minerals contributing to the liquid; C_0: concentration of the elements in the source (in ppm, except K_2O and P_2O_5, in %)

	D_0	P_L	C_0
K_2O	0.109	0.316	0.390
P_2O_5	0.070	0.217	0.115
Rb	0.032	0.103	5.594
Ba	0.118	0.340	150.859
Sr	0.118	0.340	163.605
La	0.029	0.184	5.372
Ce	0.035	0.100	13.678
Nd	0.057	0.184	7.070
Sm	0.090	0.270	1.553
Eu	0.117	0.336	0.541
Tb	0.160	0.425	0.251
Yb	0.149	0.502	0.428
Lu	0.151	0.151	0.069
Y	0.152	0.411	5.576
Zr	0.038	0.119	31.311
Hf	0.067	0.206	0.856
Nb	0.037	0.129	9.723
Ta	0.045	0.136	0.599
Th	0.011	0.071	0.465

primary melts (defined has having MgO $>$ 7% and Ni $>$ 100 ppm) found in Garrotxa, we have used the method proposed by Cebriá and López-Ruiz (1996). This method is based on the inversion of the non-modal batch melting equations of Shaw (1970). Although the actual melting process can be more complex (e.g. fractional or dynamic partial melting), those equations are still adequate to describe the variations observed in most basaltic series produced by relatively small degrees of melting from a single source (see Cebriá and López-Ruiz, 1996; Sims and DePaolo, 1997; Caroff et al., 1997). The inverse procedure is based on a two-step approach (for a detailed account of this method see Cebriá and López-Ruiz, 1996). (1) From element–element and ratio–element diagrams and a minimum number of assumptions for selected trace elements (e.g. the most incompatible element—usually Th—has $D \approx P \approx 0$, and the concentration of Yb–Lu in the source is in the range $\times 2$–$\times 4$ times the chondrites), the values of their parameters (F, D_0, P_L and C_0) are constrained within possible limits. (2) A simultaneous best-fit solution is obtained for those elements, which is then used to calculate the parameters for the remaining trace elements according to their relationships in the binary diagrams.

The results of the model (Table 2) indicate that melting degrees ranged from $F = 4$–16% from an enriched mantle source. The calculated parameters can be used to reproduce the patterns displayed by the trace elements on any binary diagram, such as the Ba/Nb–Ba/La of Fig. 6. From this calculation, it can be concluded that the linear array observed in this diagram is very likely the result of variable melting degrees and not of a mixing process. This is an interesting observation as too frequently "nearly perfect" incompatible behavior is assumed for trace elements used in ratios like the ones plotted in Fig. 6. Although this assumption can be valid for certain trace elements under some specific conditions (e.g. Hofmann et al., 1986), if used without further verification, it can lead to erroneously interpreted linear arrays as indicative of the interaction between two or more components (Hofmann et al., 1986; Sims and DePaolo, 1997). As we have seen, variable degrees of melting and small differences in the bulk distribution coefficients of incompatible elements can produce such linear variations as well.

The calculated distribution coefficients can also be considered to establish several constraints on the mineralogy of the mantle source. For example, the bulk distribution coefficients obtained for Yb confirm that garnet should be present during melting but that its proportion in the source and its contribution to the liquid are relatively low (e.g. $<$2% and $<$8%, respectively, if $D^{Yb}_{Gt/liq} = 6.4$ (Halliday et al., 1995). Unfortunately, the values of the parameters for Rb, Ba and K_2O are not sufficient to distinguish between kaersutite or phlogopite as the inferred K-bearing phase. In fact, the bulk distribution coefficients obtained for those elements can be easily reproduced with assemblages including either phlogopite as the only potassic phase or phlogopite + kaersutite. However, the relatively high partition coefficients calculated for Sr are easier to attain in the second case. Finally, the low values of the bulk distribution coefficients for K–Rb–Ba, are in agreement with the observations made for the normalized trace element diagrams, indicating that the proportion of phlogopite ± kaersutite in the source has been small

and that they have entered the melt in percentages that have allowed them to remain in the residue up to 16% melting. For example, considering the parameters calculated above (Table 2) and assuming that phlogopite is the only phase that can fractionate Rb and that $D^{Rb}_{Phl/liq} = 1.7$ (Halliday et al., 1995), the source would have ~2% phlogopite entering the liquid in a proportion under 12%.

As we have seen, the results of the modeling suggest that trace elements variations can be reproduced by partial melting from a single enriched mantle source. Several characteristics (e.g. strong Rb–Ba enrichment, presence of a K-bearing phase) also suggest that the most likely candidate for this mantle source are enriched portions of the mantle lithosphere. However, the isotopically heterogeneous character of this source, suggests that its origin may be related to the interaction of several reservoirs. To account for the origin of this mantle source, we will now mainly consider the isotopic signature of these lavas, which inherit that of their mantle source, and its relationship to the equivalent magmatism in Europe.

5.2. Isotopic constraints on the origin of the mantle source

It is generally agreed that the extensional regime developed in Europe during the Cenozoic is the main geodynamic factor controlling the generation of the so-called European Volcanic Province (see, for example, Ziegler, 1992 and references therein). From the geochemical point of view, a global explanation has recently been proposed for the apparently variable geochemistry of this volcanism. This model (see Hoernle et al., 1995; Cebriá and Wilson, 1995) suggests that the Cenozoic sodic volcanism (melilitites, nephelinites, basanites, alkali olivine basalts) of Europe, which is geochemically very similar, is generated from a common HIMU-like asthenospheric source (the Low Velocity Component (LVC) of Hoernle et al., 1995 or the European Asthenospheric Reservoir (EAR) of Cebriá and Wilson, 1995), whereas the potassic lavas (leucitites, and some leucite basanites) are likely to originate from enriched portions of the mantle lithosphere. The interaction of the LVC/EAR-derived melts with the potassic ones as the former ascend through the lithosphere produces linear trends in Sr–Nd–Pb isotopic space between the LVC/EAR composition and the potassic lavas. A possible explanation for the presence of this homogeneous reservoir and a corresponding low-velocity layer under Europe and other regions in the Central Atlantic (Hoernle et al., 1995) is the NNE-bound channeling of the Central Atlantic Plume (CAP) during the Cretaceous to present (Oyarzun et al., 1997). This would create a sublithospheric thermal and chemical anomaly that would give rise to discrete mantle diapirs and subsequent melting where relatively important extension occurred.

According to this model, any non-contaminated magmas generated from the LVC/EAR source will inherit its isotopic signature. As seen in Fig. 4, the Garrotxa lavas do not represent “pure” LVC/EAR liquids and plot in the area occupied by the Sr-enriched lavas of Massif Central. In fact, the trace element and isotopic signature of these lavas does not depart in a significant way from similar ones in Massif Central interpreted as the result of the interaction of the LVC/EAR and a lithospheric component (Cebriá and Wilson, 1995). Thus, if we accept the models proposed by Hoernle et al. (1995), Cebriá and Wilson (1995), and Oyarzun et al. (1997), the geochemical characteristics of the mantle source of the lavas from Garrotxa should be the result of the interaction between a sublithospheric component (LVC/EAR) and a lithospheric one.

If this hypothesis is correct, the distribution of the lavas of Garrotxa in trace element ratio–element (A/B–A) diagrams should follow patterns similar to those described by Sims and DePaolo (1997), in which the curves of partial melting end at the composition of the hybrid source which is located along a curve of mixing between two components. In our case, the melting curve and the composition of the hybrid source can be obtained from the melting model calculated above. Concerning the mixing curve that defines the source hybridization process, the hypothesis we are testing here implies that the composition of one of the components should be represented by LVC/EAR-derived liquids. For calculation purposes, we have assumed that they are represented by the lavas identified in the neighbor area of Calatrava on the basis of their isotopic signature (see Fig. 4). The composition of the lithospheric component is more difficult to establish as there are no constraints about it and the composition of the

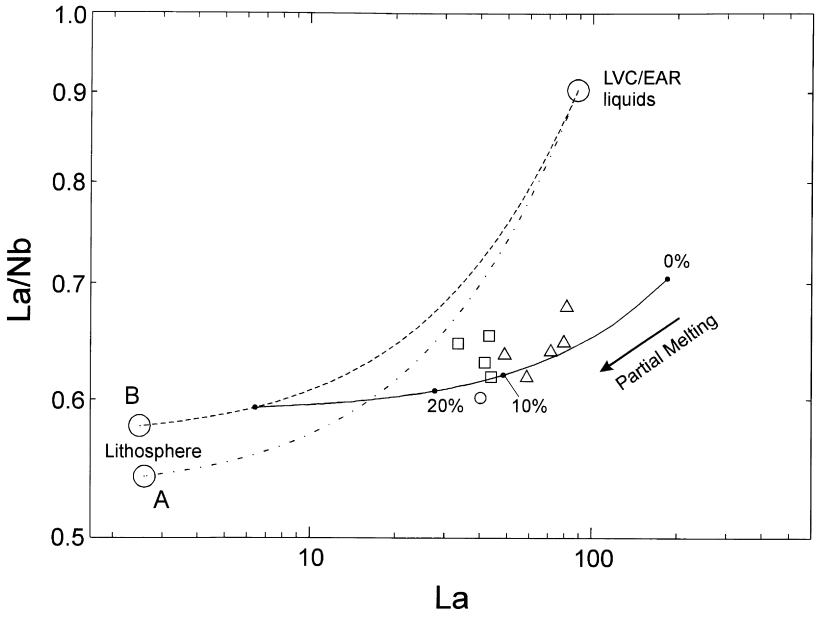

Fig. 7. Log(La/Nb)–log(La) for the primary magmas of Garroxta (symbols as in Fig. 2). The composition of the LVC/EAR-derived liquids is the average of Calatrava samples CAL-13, 19, 31 and 67 (Cebriá and López-Ruiz, 1995). The composition of the mantle lithosphere A (La = 2.6 ppm, La/Nb = 0.540) is from McDonough (1990), whereas B is a slightly modified composition (La = 2.5 ppm, La/Nb = 0.579). The solid line represents the calculated partial melting model (percentages indicate degrees of melting) from a hybrid source made up of a starting lithospheric composition (B) and LVC/EAR-derived liquids. The slight scatter of the primary lavas from the theoretical partial melting curve could be the result of the heterogeneous character of the source metasomatism.

mantle lithosphere displays very wide ranges (see, for example, McDonough, 1990). If we consider a La/Nb–La diagram (these elements are chosen for their highly incompatible behavior and their distinct values in mantle and crustal reservoirs), it can be concluded that in fact, the LVC/EAR composition is not the source of the Garrotxa lavas, and that the composition of the lithospheric component should have La $<$ 6.3 ppm and La/Nb $<$ 0.594 (Fig. 7). This condition is attained by the average values reported by McDonough (1990) for lithospheric spinel peridotites (La = 2.6 ppm and La/Nb = 0.54) providing a LVC/EAR-lithosphere mixing curve which nearly intersects the required composition of the mantle source (as defined by the melting curve). For example, a small modification of these values (La = 2.5 ppm and La/Nb = 0.579) produces a perfect fit which would imply a participation of ~5% of LVC/EAR-derived liquids in a lithospheric mantle source. Unfortunately, the lack of constraints on the actual composition of the lithospheric source in the NEVP implies that such proportion can only be considered as a first approximation. However, the above described constraints on the composition of the lithospheric component (specially the required high concentration in Nb) also imply that it should be an enriched source like those represented by some K-rich fertile lherzolites. For example, in the European domain, such peridotites have been found in the Hessian Depression (Germany) and correspond to high-K spinel peridotites with phlogopite (e.g. sample 20 of Hartmann and Wedepohl, 1990). However, the Pb isotopic ratios of such lithospheric sources are lower than those observed in the Garrotxa lavas thus suggesting that the isotopic characteristics of their source are a consequence of the second enrichment event. In fact, the addition of ~4–5% LVC/EAR liquids ($^{206}Pb/^{204}Pb = 20.0$, $^{207}Pb/^{204}Pb = 15.65$, $^{208}Pb/^{204}Pb = 39.75$; Hoernle et al., 1995, and Pb = 5 ppm, average of German primary basalts in Wilson and Downes, 1991; Wedepohl et al., 1994; Hegner et al., 1995 and Wilson et al., 1995b) into an enriched

lithospheric source similar to the above mentioned high-K peridotites (e.g. $^{206}Pb/^{204}Pb = 18.28$, $^{207}Pb/^{204}Pb = 15.56$, $^{208}Pb/^{204}Pb = 38.43$, Pb = 0.16 ppm; Amphibole-bearing spinel lherzolite Bgt6 in the work of Rosenbaum and Wilson, 1997), produces a hybrid source with the characteristics required to generate the Garrotxa lavas. This confirms that the relatively high Pb ratios of these lavas are not the consequence of the evolution during long periods of time of liquids stored into the lithosphere by an old enrichment episode, but it is inherited from the last metasomatic event by small percentages of LVC/EAR liquids.

To summarize, the petrogenetic model proposed here involves at least two enrichment stages of the lithospheric mantle previous to the melting process that produced the Garrotxa lavas: a first enrichment event, that generated enriched domains similar to those identified in other European volcanic regions as the source of high-K lavas (leucitites, leucite basanites), and a second enrichment event which should occur after the emplacement of the thermally anomalous LVC/EAR under the NEVP by Cretaceous/Paleocene time when extensional conditions started. This second stage would produce the infiltration of sublithospheric LVC/EAR liquids that were stored into the mantle lithosphere. After a short period of time, when the extensional conditions progressed, melting was triggered from the previously metasomatized mantle lithosphere involving both the stored LVC/EAR liquids and the previously enriched portions already present in the mantle lithosphere. Contrary to other areas of higher extension rates (e.g. Great Basin of Western North America; Leeman and Harry, 1993), the absence of asthenospheric melts in the NEVP implies that the rates of extension were always low, which also agrees with the small volume of magmas generated. The lavas produced from this hybrid source will therefore show trace element variations in accordance with partial melting from a single mantle source with a relatively heterogenous isotopic signature. They will also show a geochemical signature intermediate between the LVC/EAR and the enriched lithosphere. An additional consequence of this model, is that the inferred presence of garnet in the source is not necessarily a feature of the mantle lithosphere and could represent a geochemical relic of the second enrichment event which is produced by liquids generated at deeper (sublithospheric) levels. This situation has already been suggested to explain the presence of spinel-clinopyroxene clusters that substitute garnet at lithospheric levels in mantle xenoliths from the Rhön (Witt-Eickschen and Kramm, 1997). Other characteristics of the lavas, like the strong enrichment in Rb, Ba or the inferred presence of a K-bearing phase, can be attributed to both enrichment events since K-bearing phases are a common feature of enriched portions of the lithosphere and these phases have also been reported in the mantle source of LVC/EAR-derived liquids (e.g. Wilson and Downes, 1991; Cebriá and López-Ruiz, 1995). This model is in agreement with the presence of pervasive LVC/EAR-like veins in mantle lithosphere xenoliths as reported in the Carpathian–Pannonian region (Rosenbaum and Wilson, 1997), suggesting that the infiltration/storage of LVC/EAR-derived melts in the lithosphere is a common feature in the European domain.

6. Geodynamic scenario

The geochemical model presented in this paper for the Garrotxa volcanism implies the existence of at least two different mantle lithosphere enrichment events beneath this region before volcanics were finally extruded. (1) A first event that is responsible for the presence of highly enriched domains within the mantle lithosphere; and (2) a recent event characterized by the infiltration of LVC/EAR-derived melts. The geodynamic history of the lithosphere in the NEVP has several characteristics that can help to explain the above-identified events.

Following the Variscan compressions and build-up of the orogen in the Pyrenean area (Fig. 8a), this realm underwent major extensional collapse during the Permo-Carboniferous (Fig. 8b) accompanied by magmatic activity (volcanics, dyke intrusions, plutonism; Vissers, 1992), thus rejuvenating the lower crust and generating a deep-seated, weak and permanently buoyant underplated anomalous lithosphere (as suggested for the Late Variscan European belt by Costa and Rey, 1995). This extensional process was accompanied by mantle upwelling so it can account for the first enrichment event of the mantle lithosphere under the NEVP required by the geochemical model.

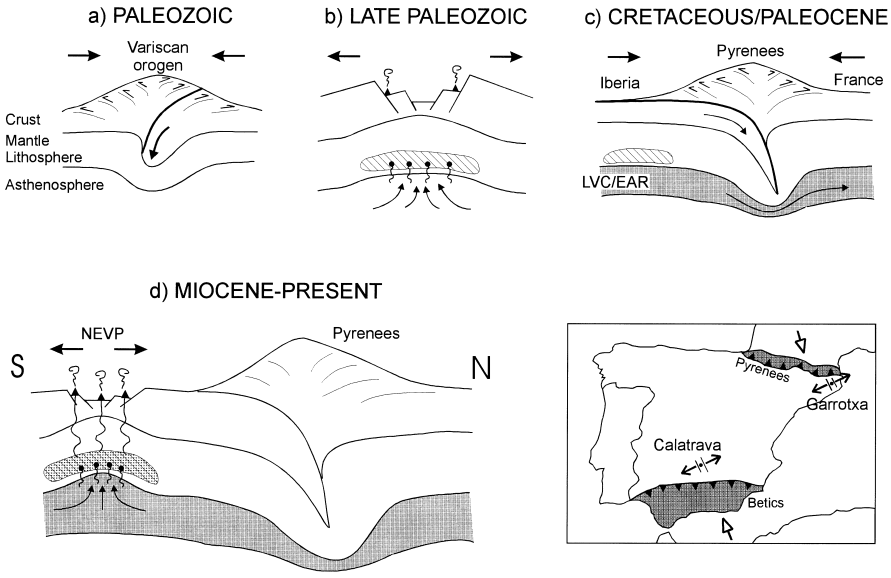

Fig. 8. Schematic diagram showing the general geotectonic evolution of the Pyrenean realm and its foreland since the Variscan depicting the successive events that preconditioned the final extrusion of Miocene to Quaternary volcanics in the NEVP. Cross-sections not to scale. (a) Variscan compressions leading to the buildup of a Paleozoic belt in the future Pyrenean realm. (b) Late Variscan extensional collapse of the previous overthickened belt, accompanied by thinning of the lithosphere, first enrichment episode of the mantle lithosphere (striped area) and magmatism. (c) Cretaceous/Paleocene buildup of the Pyrenean belt accompanied by intracontinental subduction of the Iberian lithosphere beneath France. This figure also shows the sublithospheirc NNE-directed channeling of the LVC/EAR. (d) Miocene to present extension and volcanism in Garrotxa in the Iberian foreland as a response to relic compression in the Pyrenean belt. The extrusion of the NEVP volcanics is preceded by a second enrichment episode of the mantle lithosphere (shaded and striped area) in relation to a mantle diapir from the LVC/EAR. The inset shows the similar geotectonic environments for two NW–SE-oriented recent volcanic provinces (Garrotxa and Calatrava) in Spain related to Late Alpine relic compressions.

From the Jurassic/Cretaceous until the Cenozoic, large-scale NNE-directed sublithospheric mantle channeling from a Triassic/Jurassic Central Atlantic superplume (Oyarzun et al., 1997) reached the Iberian Peninsula and Central Europe, generating a sublithospheric HIMU-like reservoir (the LVC/EAR) identified both by tomographies and geochemically (Hoernle et al., 1995; Cebriá and Wilson, 1995). In the case of the NEVP, this thermal and chemical anomaly was not able to produce magmatism until the Cenozoic, due to the geodynamic conditions that prevailed in the area. During the Jurassic/Cretaceous, the Iberian Peninsula rotated anti-clockwise opening the Bay of Biscay at the expense of the convergence between Iberia and France. After a long time of oblique convergence, Iberia and France finally collided during the Cretaceous/Tertiary giving rise to the Pyrenean orogen (Olivet, 1996; Fig. 8c) accompanied by northward-directed intracontinental subduction of the Iberian continental lithosphere beneath France. It is plausible that the north-deepening relic intracontinental subduction zone beneath the Pyrenees might have contributed to accumulate some of the NNE-directed sublithospheric mantle flow, preferentially beneath the NEVP, thus favoring the adiabatic ascent of a discrete mantle diapir and triggering the second identified event of mantle lithosphere enrichment by the infiltration of LVC/EAR-derived liquids (Fig. 8d).

Like for the other Cenozoic volcanic regions in Iberia and Europe, volcanism in the NEVP only occurred when extensional conditions prevailed. In this area, the extension and extrusion of magmas is related first (sectors of Ampurdán and Selva) to normal faulting that follows the trends of the NE–SW-oriented Cenozoic European rift system. This is followed in Garrotxa by NW–SE faulting

related to relic compressional stresses associated to the final convergence of the Alpine orogens (i.e. by the indentation of the Pyrenees; Fig. 8c), similarly to what happens in Calatrava (indentation of the Betic Cordilleras) or southern France (indentation of the Alps). Thus, the volcanic activity along the NEVP might represent a far-reaching/deep-seated consequence of the anomalous late Paleozoic to present evolution of the lithosphere beneath the region. Furthermore, it is conceivable that this region constituted, since the late Paleozoic, a "lithospheric weak zone" which facilitated the break-up of the Pyrenean foreland precisely in this region by the end of the Alpine compressions.

7. Conclusions

The Quaternary leucite basanites, nepheline basanites and olivine basalts of Garrotxa derived by melting degrees between 4 and 16% from a single enriched lithospheric mantle source with an heterogeneous Sr–Nd–Pb isotopic signature.

The geochemical characteristics of this mantle source are interpreted as the result of at least two metasomatic events in the mantle lithosphere: a first one which is responsible for the presence of highly enriched domains, and a second one that produced the infiltration of LVC/EAR-like liquids derived from a sublithospheric mantle source. The resulting lithospheric source would then melt generating liquids with characteristics intermediate between the LVC/EAR ones and the enriched portions of the lithosphere. This process implies that the resulting magmas show homogeneous partial melting patterns concerning trace elements but a more heterogeneous isotopic signature, which reflects the interaction between the lithospheric enriched domains and the LVC/EAR-derived liquids. Similarly, some trace element characteristics, like the relative depletion in HREE due to the presence of residual garnet, are possible geochemical relics of the generation of the sublithospheric LVC/EAR liquids whereas other characteristics (e.g. the Rb–Ba enrichment or the inferred presence of a potassic phase) are fingerprints of the enriched lithospheric domains.

The geochemical characteristics of the NEVP volcanics might be explained by the long-lived evolution of the mantle lithosphere beneath the region. The first enrichment event could be related to the Late Paleozoic extensional collapse of the protoPyrenean belt and the second one to the beginning of extensional processes in the Cenozoic. This last enrichment event would be closely associated to the localized ascent of a mantle diapir from the LVC/EAR (active beneath the region since the Cretaceous/Tertiary). The Garrotxa volcanism is related to later NW–SE-oriented extensional faulting associated to relic Pyrenean compressional stresses.

Acknowledgements

J.M.C. wishes to thank Dr M. Wilson for her support and encouragement during his stay at the University of Leeds. Also thanks to Dr R. Cliff, Dr J. Rosenbaum, P. Guise and R. Green for their help during the analytical work at the Geochronology Laboratory of the School of Earth Sciences at Leeds University (UK). The authors also wish to acknowledge the comments by Dr C. Chauvel on an earlier version of this manuscript and the helpful revisions made by Prof. Leeman and Prof. Verma. This work was financially supported by DGESIC project PB95-0107.

References

Alibert, C., Leterrier, J., Panasiuk, M., Zimmermann, J.L., 1987. Trace and isotope geochemistry of the alkaline Tertiary volcanism in southwestern Poland. Lithos 20, 311–321.

Araña, V., Aparicio, A., Martín-Escorza, C., Garcia-Cacho, L., Ortiz, R., Vaquer, R., Barberi, F., Ferrara, G., Albert, J., Gassiot, X., 1983. El volcanismo neógeno-cuaternario de Catalunya: caracteres estructurales, petrológicos y geodinámicos. Acta Geol. Hisp. 18, 1–17.

Benito-García, B., López-Ruiz, J., Turi, B., 1992. Valores $\delta\sigma_{18}$ de los basaltos alcalinos de la región volcánica de Olot, La Garrotxa, Cataluña. Estudios Geol. 48, 43–6.

Blusztajn, J., Hart Sr, S.R., 1989. Nd, and Pb isotopic character of Tertiary basalts from southwest Poland. Geochim. Cosmochim. Acta 53, 2689–2696.

Briot, D., Cantagrel, J.M., Dupuy, C., Harmon, R.S., 1991. Geochemical evolution in crustal magma reservoirs: trace-element and Sr–Nd–O isotopic variations in two continental intraplate series at Monts Doré, Massif Central, France. Chem. Geol. 89, 281–303.

Caroff, M., Maury, R.C., Guille, G., Cotten, J., 1997. Partial melting below Tubuai (Austral Islands, French Polynesia). Contrib. Miner. Petrol. 127, 369–382.

Cebriá, J.M., López-Ruiz, J., 1995. Alkali basalts and leucitites in an extensional intracontinental plate setting: the Late Cenozoic Calatrava Volcanic Province (Central Spain). Lithos 35, 27–46.

Cebriá, J.M., Wilson, M., 1995. Cenozoic mafic magmatism in Western/Central Europe: a common european asthenospheric reservoir?. Terra Nova Abs. Sup. 7, 162.

Cebriá, J.M., López-Ruiz, J., 1996. A refined method for trace element modelling of nonmodal batch partial melting processes: the Cenozoic continental volcanism of Calatrava, Central Spain. Geochim. Cosmochim. Acta 60, 1355–1366.

Chauvel, C., Jahn, B.M., 1984. Nd–Sr isotope and REE geochemistry of alkali basalts from the Massif Central France. Geochim. Cosmochim. Acta 48, 93–110.

Chauvel, C., Hofmann, A.W., Vidal, Ph., 1992. HIMU-EM: the French Polynesian connection. Earth Planet. Sci. Lett. 110, 99–119.

Costa, S., Rey, P., 1995. Lower crustal rejuvenation and growth during post-thickening collapse: insights from a crustal cross-section through a Variscan metamorphic core complex. Geology 23, 905–8.

Díaz, N., Gimeno, D., Losantos, M., Segura, C., 1996. Las traquitas de Arenys d'Empordà (Alt Empordà, NE de la Península Ibérica): características generales. Geogaceta 20, 572–5.

Doblas, M., Oyarzun, R., 1989. Neogene extensional collapse in the western Mediterranean (Betic-Rif Alpine orogenic belt): implications for the genesis of the Gibraltar Arc and magmatic activity. Geology 17, 430–3.

Doblas, M., Oyarzun, R., 1990. The Late Oligocene-Miocene opening of the North Balearic Sea (Valencia Basin, western Mediterranean): a working hypothesis involving mantle upwelling and extensional detachment tectonics. Marine Geol. 94, 155–163.

Donville, B., 1973a. Ages potassium–argon des vulcanites du Haut-Ampurdan (Nord–Est de l'Espagne). Implications stratigraphiques. C.R. Acad. Sci. Paris 276, 2497–2500.

Donville, B., 1973b. Ages potassium-argon des vulcanites du Bas-Ampurdan (Nord-Est de l'Espagne). C.R. Acad. Sci. Paris 276, 3253–6.

Donville, B., 1973c. Ages potassium–argon des roches volcaniques de la depression de La Selva (Nord-Est de l'Espagne). C.R. Acad. Sci. Paris 277, 1–4.

Downes, H., 1984. Sr and Nd isotope geochemistry of co-existing alkaline magma series, Cantal, Massif Central, France. Earth Planet. Sci. Lett. 69, 321–334.

Guérin, G., Benhamou, G., Mallarach, J.M., 1986. Un exemple de fusió parcial en medi continental. El vulcanisme quaternari de Catalunya. Vitrina 1, 20–6.

Halliday, A.N., Lee, D.C., Tommasini, S., Davies, G.R., Paslick, C.R., Fitton, J.G., James, D.E., 1995. Incompatible trace elements in OIB and MORB and source enrichment in the sub-oceanic mantle. Earth Planet. Sci. Lett. 133, 379–395.

Harmon, R.S., Hoefs, J., 1995. Oxygen isotope heterogeneity of the mantle deduced from global 18O systematics of basalts from different geotectonic settings. Contrib. Mineral. Petrol 120, 95–114.

Hart, S.R., 1988. Heterogeneous mantle domains: signatures, genesis and mixing chronologies. Earth Planet. Sci. Lett. 90, 273–296.

Hartmann, G., Wedepohl, K.H., 1990. Metasomatically altered peridotite xenoliths from the Hessian Depression (Northwest Germany). Geochim. Cosmochim. Acta 54, 71–86.

Hegner, E., Walter, H.J., Satir, M., 1995. Pb-Sr-Nd isotopic compositions and trace element geochemistry of megacrysts and melilitites from the Tertiary Urach volcanic field: source composition of small volume melts under SW Germany. Contrib. Mineral. Petrol 122, 322–335.

Hoefs, J., 1997. Stable Isotope Geochemistry. 4th ed., Springer, New York (p. 210).

Hoernle, K., Zhang, Y.S., Graham, D., 1995. Seismic and geochemical evidence for large-scale mantle upwelling beneath the eastern Atlantic and western and central Europe. Nature 374, 34–9.

Hofmann, A.W., Jochum, K.P., Seufert, M., White, W.M., 1986. Nb and Pb ind oceanic basalts: new constraints on mantle evolution. Earth Planet. Sci. Lett. 79, 33–45.

Jung, S., Masberg, P., 1998. Major- and trace-element systematics and isotope geochemistry of Cenozoic mafic volcanic rocks from the Vogelsberg (central Germany). Constraints on the origin of continental alkaline and tholeiitic basalts and their mantle sources. J. Volcanol. Geotherm. Res. 86, 151–177.

Kyser, T.K., 1986. Stable isotope variations in the mantle. In: Valley, J.W., Taylor, H.P., O'Neil, J.R. (Eds.). Stable Isotopes in High Temperature Geological Processes, pp. 141–164.

Leeman, W.P., Harry, D.L., 1993. A binary source model for extension-related magmatism in the Great Basin, Western North America. Science 262, 1550–4.

López-Ruiz, J., Rodríguez-Badiola, E., 1985. La región volcánica Mio-Pleistocena del NE de España. Estudios Geol. 41, 105–126.

López-Ruiz, J., Cebriá, J.M., Doblas, M., Oyarzun, J., Hoyos, M., Martín, C., 1993. Cenozoic intra-plate volcanism related to extensional tectonics at Calatrava, central Iberia. J. Geol. Soc. London 150, 915–922.

Martí, J., Mallarach, J.M., 1987. Erupciones hidromagmáticas en el volcanismo cuaternario de Olot (Girona). Estudios Geol. 43, 31–40.

Martí, J., Mitjavila, J., Roca, E., Aparicio, A., 1992. Cenozoic magmatism of the Valencia trough (western Mediterranean): relationship between structural evolution and volcanism. Tectonophysics 203, 145–165.

McDonough, W.F., 1990. Constraints on the composition of the continental lithosphere mantle. Earth Planet. Sci. Lett. 101, 1–18.

Mertes, H., Schmincke, H.U., 1985. Mafic potassic lavas of the Quaternary West Eifel volcanic field. I. Major and trace elements. Contrib. Miner. Petrol. 89, 330–345.

Olivet, J.L., 1996. La cinématique de la plaque Ibérique. Bull. Centres Recherche, Exploration–Production, Elf-Aquitaine 20, 131–195.

Oyarzun, R., Doblas, M., López-Ruiz, J., Cebriá, J.M., 1997. Opening of the central Atlantic and asymmetric mantle upwelling phenomena: implications for long-lived magmatism in western North Africa and Europe. Geology 25, 727–730.

Rosenbaum, J.M., Wilson, M., 1997. Multiple enrichment of the Carpathian–Pannonian mantle: Pb–Sr–Nd isotope and trace element constraints. J. Geophys. Res. 102, 14947–14961.

Shaw, D.M., 1970. Trace element fractionation during anatexis. Geochim. Cosmochim. Acta 34, 237–243.

Sims, K.W.W., DePaolo, D.J., 1997. Inferences about mantle magma sources from incompatible element concentration ratios in oceanic basalts. Geochim. Cosmochim. Acta 61, 765–784.

Solé-Sabarís, L., 1962. Observaciones sobre la edad del volcanismo gerundense. Mem. R. Acad. Ciencias Artes Barcelona 34, 359–372.

Solé-Sugrañés, L., 1978. Alineaciones y fracturas en el sistema catalán según las imágenes Landsat-1. Tecniterrae 22, 6–16.

Solé-Sugrañés, L., Juliá, R., Anadón, P., 1984. El sistema de fosas neógenas del NE de la península ibérica. In: El borde mediterráneo español: evolución del orógeno bético y geodinámica de las depresiones neógenas. C.S.I.C., Granada, pp. 87–91.

Sun, S.S., McDonough, W.F., 1989. Chemical and isotopic systematics of oceanic basalts: implications for mantle composition and processes. In: Saunders, A.D., Norry, M.J. (Eds.). Magmatism in the Ocean Basins, pp. 313–345.

Vidal, Ph., 1992. Mantle: more HIMU in the future?. Geochim. Cosmochim. Acta 56, 4295–9.

Vissers, R.L.M., 1992. Variscan extension in the pyrenees. Tectonics 11, 1369–1384.

Weaver, B.L., 1991. The origin of ocean island basalt end-member compositions: trace element and isotopic constraints. Earth Planet. Sci. Lett. 104, 381–397.

Wedepohl, K.H., Gohn, E., Hartmann, G., 1994. Cenozoic alkali basaltic magmas of western Germany and their products of differentiation. Contrib. Mineral. Petrol. 115, 253–278.

Wilson, M., Downes, H., 1991. Tertiary–Quaternary extension-related alkaline magmatism in western and central Europe. J. Petrol. 32, 811–849.

Wilson, M., Downes, H., Cebriá, J.M., 1995a. Contrasting fractionation trends in coexisting continental alkaline magma series; Cantal, Massif Central, France. J. Petrol. 36, 1729–1753.

Wilson, M., Rosenbaum, J.M., Dunworth, E.A., 1995b. Melilitites: partial melts of the thermal boundary layer? Contrib. Miner. Petrol. 119, 181–196.

Witt-Eickschen, G., Kramm, U., 1997. Mantle upwelling and metasomatism beneath Central Europe: Geochemical and isotopic constraints from mantle xenoliths from the Rhön (Germany). J. Petrol. 38, 479–493.

Wörner, G., Zindler, A., Staudigel, H., Schmincke Sr, H.U., 1986. Nd and Pb isotope geochemistry of Tertiary and Quaternary alkaline volcanics from West Germany. Earth Planet. Sci. Lett. 79, 107–119.

Zeyen, H.J., Banda, E., Klingelé, E., 1991. Interpretation of magnetic anomalies in the volcanic area of northeastern Spain. Tectonophysics 192, 201–210.

Zindler, A., Hart, S., 1986. Chemical Geodynamics. Ann. Rev. Earth Planet. Sci. 14, 493–571.